Hindawi Publishing Corporation
Physics Research International
Volume 2011, Article ID 496057, 7 pages
doi:10.1155/2011/496057

Research Article

Effects of Pressure Drops on the Performance Characteristics of Air Standard Otto Cycle

Mahmoud Huleihil

Academic Institute for Training Arab Teachers (AITAT), Beit Berl Academic College, Doar Beit Berl 44905, Israel

Correspondence should be addressed to Mahmoud Huleihil, cs.berl@gmail.com

Received 16 September 2010; Accepted 25 May 2011

Academic Editor: Frank Tsui

The effects of pressure drops on the performance characteristics of the air standard Otto cycle are reported. The pressure drops are assumed as constant values independent of the engine size. It has been shown that the pressure drops to about 60% of the maximum pressure in the ideal cycle (Curto-Risso et al., 2008). Three different models are studied: constant pressure model, reversible adiabatic expansion model and polytropic expansion model. The findings of this study show that, at this level of pressure drop, the maximum efficiency of the Otto cycle is reduced by 15% approximately based on the constant pressure model. The combined effect of pressure drop with other modes of irreversibility, for example, internal irreversibility and heat leaks, could reduce the maximum efficiency into very low values (approximately 30%). The reversible adiabatic model predicts reduction of 13% in efficiency at 40% pressure drop levels but at the price of zero power production. On the other hand, the polytropic expansion model predicts 40% reduction in efficiency for the same level of pressure drop (40%). All three models show that the power output is very sensitive to pressure drop.

1. Introduction

Finite time thermodynamics (FTT) is a nonequilibrium theory. Its aim is to provide performance bounds and extremes for irreversible thermodynamic processes [1]. FTT has been used extensively to analyze the performance characteristics of the air standard Otto cycle [2–12]. What is the theoretical efficiency of a heat engine producing the maximum possible work per cycle consistent with its operating temperature range? This question was raised and had been answered using four models of reversible heat engine cycles (Otto, Joule Brayton, Diesel, and Atkinson) [2]. The derived expression for efficiency at maximum power production is given by the Curzon-Ahlborn expression: $\eta_{CA} = 1 - \sqrt{T_{min}/T_{max}}$, where T_{min} is the minimal temperature and T_{max} is the maximal temperature between them the heat engine runs. It is important to stress that the maximum efficiency is not affected by the assumptions of the analysis. Heat engines are naturally characterized by their power efficiency curves. Real heat engines suffer from different modes of irreversibility, for example, finite heat transfer rates, friction (internally or externally), heat leaks, and real equation of state [13]. These modes of irreversibility affect not only the maximum power production but also the maximum efficiency. The power efficiency curves trace a loop shape thus, the power and efficiency vanish at two extremes: at very slow and very fast operations (similar to open voltage and short circuit limits in an electrical circuit).

The method of FTT with the method of optimal control theory has been applied to determine the optimal piston trajectory for successively idealized models of the Otto cycle [3]. The optimal path has significantly smaller losses from friction and heat leaks than the path with conventional piston motion and the same loss parameters. In their study the researchers showed that the efficiency could be increased by 10%.

Different effects have been studied on the standard air Otto cycle.

FTT Bounds about the efficiency at maximum power production of an air standard Otto cycle were found under the effects of cylinder wall heat transfer [4].

The effects of engine speed on the characteristic performance of an air standard Otto cycle were analyzed [5]. The results showed that the optimal compression ratio

corresponding to the maximum power output point remains constant with increased engine speed.

Performance analyses of an irreversible Otto cycle were considered using finite time thermodynamics [6]. In their study, they considered different models of losses, for example, friction, heat leaks, heat transfer loss, and internal irreversibly (no isentropic processes). The results showed that the power output decreases with the increase of the internal irreversibility whether there is or not a friction loss. Similarly, the power output decreases with the increase of friction loss whether or not there is internal irreversibility and there is no effect of heat transfer loss and heat leak rate.

The temperature-dependent specific heat and isentropic efficiencies were considered, and there effects on the power output and on the thermal efficiency of an air standard Otto cycle were studied [7].

The effect of the variable specific heat ratio on the performance of on endoreversible Otto cycle was studied [8]. It has been reported that the effects of the temperature dependent specific heat ratio of the working fluid on the endoreversible cycle performance are significant and should be considered in practical cycle analysis and design. In different studies [9] considered the effect of the combustion efficiency and the variable volumetric efficiency and [12] considered the effect of volumetric efficiency on the cycle efficiency. It has been found that these effects are significant and could not be neglected.

The effects of cylinder wall heat transfer and global losses were lumped in a friction-like term on performance of different cycles (Diesel, Otto, Atkinson, and Brayton) [11]. In their study, they derived a universal relation between power output and the compression ratio, between the thermal efficiency and the compression ratio and the optimal relation between power output and efficiency for the cycles considered.

Theoretical and simulated models for an irreversible Otto cycle were developed [14]. In their study they showed that a finite time thermodynamics model of an irreversible Otto cycle is suitable to reproduce performance results of a real spark ignition heat engine. They showed that a theoretical Otto cycle with different modes of irreversibility arising from friction, heat transfer through the cylinder walls, and internal losses properly produces simulation results by considering extreme temperatures and mass inside the cylinder as functions of the rotational engine speed. From the simulation plots of P-V curve, one observes that the maximum pressure is about 60% of the maximal pressure of the ideal Otto cycle.

Cyclic variations in combustion, inside Otto engine, accounting for partial burning and misfire are extensively considered by Heywood [10]. Since the pressure development is uniquely related to the combustion process, substantial variations in the combustion process on a cycle-by-cycle basis are occurring. An example of the cycle-by-cycle variations in cylinder pressure and the variations in mixture burning rate cause them are shown in [10]. One could observe that the variations in maximum pressure are approximately 50%. Thus, imperfections in the combustion process (e.g., incomplete combustion, longer combustion times, higher heat leaks, etc.) reduce both the power and efficiency of the Otto engine.

In this study, the effect of pressure drop on the performance analysis of an air standard cycle is considered.

The paper is arranged as follows: in Section 2 the considered model for standard air Otto cycle with pressure drop is introduced, in Section 3 numerical examples are discussed, and summary and conclusions are considered in Section 4.

2. Air Standard Otto Cycle with Pressure Drop

2.1. Constant Pressure Model. Consider the air standard Otto cycle with two isentropic branches (compression and expansion) and with two constant volume heat addition and rejection (see Figure 1). Process $1 \to 2s$ is an isentropic compression branch, process $2s \to 3$ is a constant volume heat addition branch, process $3 \to 4s$ is an isentropic expansion branch, and $4s \to 1$ is a constant volume heat rejection branch. The pressure drops deviations from the ideal cycle are depicted by points $3'$, $3''$, $1'$, and $1''$ in Figure 1. On the other hand, internal irreversibility is modeled via isentropic efficiencies η_c and η_e (will be defined later in this section similar to the definition given in [9]) and a constant heat leak term to account for heat loss from the hot side to the cold side at extreme conditions.

The thermodynamic properties along the isentropic branches are related via the following equations.

Pressure-Volume Relation (Isentropic Branch)

$$PV^k = \text{const}, \tag{1}$$

where P is the pressure, V is the volume, and k is the ratio of the specific heat at constant pressure to the specific heat at constant volume of the working fluid.

Temperature-Volume Relation (Isentropic Branch)

$$TV^{k-1} = \text{const}, \tag{2}$$

where T is the temperature of the working fluid.

Pressure-Temperature Relation (Constant Volume Branch). The thermodynamics along the constant volume branches are related according the following relation:

$$\frac{P}{T} = \text{const}. \tag{3}$$

Volume-Temperature Relation (Constant Pressure Branch)

$$\frac{V}{T} = \text{const}. \tag{4}$$

For given thermodynamic properties at point 1 (P_1, V_1, T_1), the volume V_{2s} at point 2s, and the temperature T_3 at point 3, it is possible to find the other properties. By applying

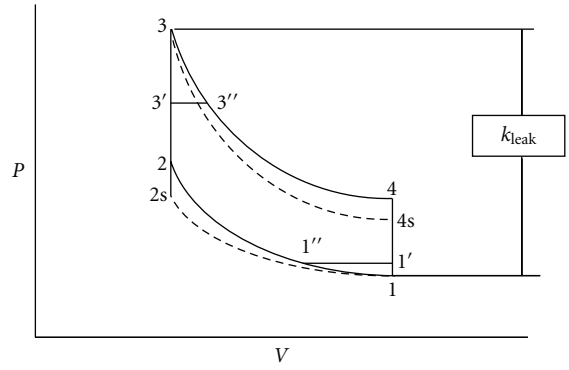

Figure 1: Schematics of the air standard Otto cycle with different modes of irreversibility: cycle $1 \to 2s \to 3 \to 4s \to 1$ represents the ideal Otto cycle; pressure drop is represented by points $1'$, $1''$, $3'$, and $3''$; isentropic losses are represented by points 2 and 4, and heat leak is represented by the heat leak coefficient k_{leak}.

relations (1)–(4) it is possible to find the pressures and temperatures at the different points. Temperature T_{2s} is given by

$$T_{2s} = T_1 r^{k-1}, \tag{5}$$

where r is the compression ratio ($r \equiv V_1/V_2$), and T_{4s} is given by:

$$T_{4s} = \frac{T_3}{r^{k-1}}. \tag{6}$$

Along the isentropic branches, the heat transfer is zero. The heat addition per unit mass along the constant volume branch $2s \to 3$ is given by

$$Q_{\text{in}} = c_v(T_3 - T_{2s}), \tag{7}$$

and the heat rejection per unit mass along the constant volume branch $4s \to 1$ is given by

$$Q_{\text{out}} = c_v(T_{4s} - T_1). \tag{8}$$

The work output per cycle w is calculated from the first law of thermodynamics and is given by

$$W = Q_{\text{in}} - Q_{\text{out}}. \tag{9}$$

Finally, the thermal efficiency η is defined as the ratio of the work output to the heat input and is given by

$$\eta = \frac{W}{Q_{\text{in}}}. \tag{10}$$

After algebraic manipulations and normalizing the heat input and rejection, it is possible to recast the normalized heat input q_{in} in the following form:

$$q_{\text{in}} = \frac{Q_{\text{in}}}{c_v T_3} = 1 - \tau\, r^{k-1}, \tag{11}$$

and the normalized heat rejection q_{out} is given by

$$q_{\text{out}} = \frac{Q_{\text{out}}}{c_v T_3} = \frac{1}{r^{k-1}} - \tau. \tag{12}$$

Accordingly, the normalized work output w is given by

$$w = \frac{W}{c_v T_3} = \left(1 - \tau\, r^{k-1}\right)\left(1 - \frac{1}{r^{k-1}}\right), \tag{13}$$

and finally the thermal efficiency is given by

$$\eta = 1 - \frac{1}{r^{k-1}}. \tag{14}$$

In order to model the pressure drop effect on the performance characteristics of the air standard Otto cycle, we introduce the following relations (see Figure 1 for more details).

The pressure at point $3'$ is defined as follows:

$$P_{3'} = \varepsilon_3 P_3, \tag{15}$$

where ε_3 is the pressure drop ratio at point 3 and its value falls in the range (0-1).

Similarly, the pressure at point $1'$ is defined as follows:

$$P_{1'} = \frac{P_1}{\varepsilon_1}, \tag{16}$$

where ε_1 is the pressure drop ratio at point 1 and its value falls in the range (0-1).

Using definitions (15) and (16) along with the thermodynamic relation, it is possible to calculate the temperatures at points $1'$, $1''$, $3'$, and $3''$. The temperatures at these are given as follows:

$$\begin{aligned} T_{1'} &= \frac{T_1}{\varepsilon_1}, \\ T_{1''} &= \varepsilon^{(1/k)-1} T_1, \\ T_{3'} &= \varepsilon_3 T_3, \\ T_{3''} &= \varepsilon^{1-(1/k)} T_3. \end{aligned} \tag{17}$$

The isentropic efficiencies are defined as follows.

The isentropic compression efficiency is given by the following definition:

$$\eta_c = \frac{T_{2s} - T_1}{T_2 - T_1}, \tag{18}$$

and the isentropic expansion efficiency is given by the following definition:

$$\eta_e = \frac{T_4 - T_3}{T_{4s} - T_3}. \tag{19}$$

The heat leak term is assumed to be constant and is given by the following expression:

$$Q_{\text{leak}} = k_{\text{leak}}(T_3 - T_1). \tag{20}$$

The heat input to the heat engine considering the three different modes of irreversibility (pressure drop, internal irreversibility, and heat leak) is given by

$$Q_{\text{in}} = c_v(T_{3'} - T_2) + c_p(T_{3''} - T_{3'}) - Q_{\text{leak}}, \tag{21}$$

and the heat rejection from the heat engine is given by

$$Q_{\text{out}} = c_v(T_4 - T_{1'}) + c_p(T_{1'} - T_{1''}) - Q_{\text{leak}}. \tag{22}$$

The normalized heat input to the heat engine $q_{\text{in}'}$ after some algebraic manipulation is given by

$$q_{\text{in}'} = A - \frac{\tau}{\eta_c} r^{k-1}, \tag{23}$$

where A is given by

$$A = \varepsilon_3 - \tau + \frac{\tau}{\eta_c} + \kappa\left(\varepsilon_3^{1-(1/k)} - \varepsilon_3\right) - \kappa_{\text{leak}}(1 - \tau). \tag{24}$$

Similarly, the normalized heat rejection $q_{\text{out}'}$ from the heat engine is given by

$$q_{\text{out}'} = \frac{\eta_e}{r^{k-1}} - B, \tag{25}$$

where B is given by

$$B = -\left(1 - \eta_e - \frac{\tau}{\varepsilon_1} + \kappa\tau\left(\frac{1}{\varepsilon_1} - \varepsilon_1{}^{(1/k)-1}\right)\right) - \kappa_{\text{leak}}(1 - \tau). \tag{26}$$

The normalized work output for the irreversible heat engine w' is given by

$$w' = q_{\text{in}'} - q_{\text{out}'}, \tag{27}$$

and finally the thermal efficiency is given by

$$\eta' = \frac{w'}{q_{\text{in}'}}. \tag{28}$$

In the following section, equations (23)–(28) are used to present the efficiency and power output for different values of the loss coefficients.

2.2. Reversible Adiabatic Expansion Model. In this model the pressure drop at point 3 reduces the maximum temperature to $T_{3'}$. The working fluid expands adiabatically to point 4s′ (see Figure 5). The temperature at point 4s′ is given by

$$T_{4s'} = \frac{\varepsilon_3 T_3}{r^{k-1}}. \tag{29}$$

The heat input to the heat engine system $Q_{\text{in,s}}$ is given by

$$Q_{\text{in,s}} = c_v(T_{3'} - T_{2s}) = c_v(\varepsilon_3 T_3 - T_{2s}). \tag{30}$$

Similarly, the heat rejection from the heat engine system $Q_{\text{out,s}}$ is given by

$$Q_{\text{out,s}} = c_v(T_{4s'} - T_1). \tag{31}$$

The net work output and efficiency are found from (9) and (10), respectively.

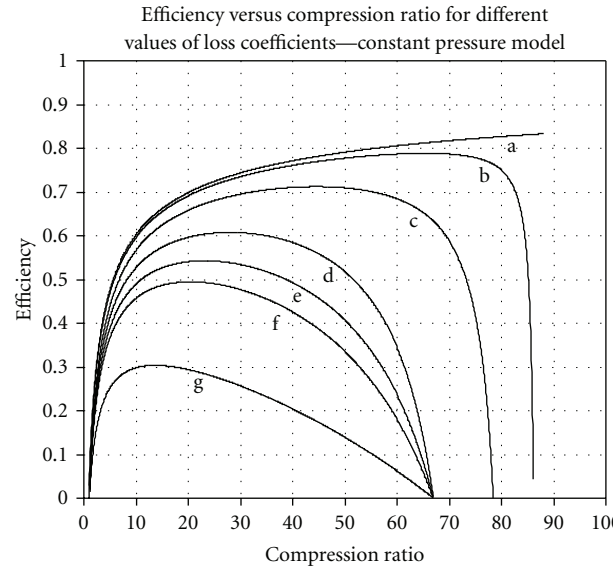

Figure 2: Efficiency versus compression ratio is plotted for different values of loss coefficients (pressure drop at point 1—ε_1, pressure drop at point 3—ε_3, compression isentropic efficiency—η_c, expansion isentropic efficiency η_e, and heat leak coefficient—k_{leak}). The loss coefficients' values are (in the same order that appeared above) (a) 1, 1, 1, 1, 0; (b) 0.8, 0.8, 1, 1, 0; (c) 0.6, 0.6, 1, 1, 0; (d) 0.6, 0.6, 0.97, 0.97, 0; (e) 0.6, 0.6, 0.97, 0.97, 0.05; (f) 0.6, 0.6, 0.97, 0.97, 0.1; (g) 0.6, 0.6, 0.97, 0.97, 0.5.

2.3. Polytropic Expansion Model. The assumption of this model is that the working fluid expands following a polytropic branch with exponent n (PV^n = const.) from point 3′ to point 4s. In order to fulfill the extreme temperatures $T_{3'}$ and $T_{4s'}$ the following relation must be fulfilled:

$$n = k + \frac{\ln(\varepsilon_3)}{\ln(r)}. \tag{32}$$

Then the heat input to the heat engine system $Q_{\text{in},n}$ is given by

$$Q_{\text{in},n} = c_v(T_{3'} - T_{2s}) + c_v\left(\frac{k-n}{n-1}\right)(T_{3'} - T_{4s}). \tag{33}$$

The heat rejection from the heat engine system, the net work output, and the thermal efficiency are given by (8)–(10) along with (32) and (33).

3. Numerical Examples

In this section typical values of thermodynamic properties are used. The heat engine is assumed to work between $T_1 = 300\,\text{K}$ and $T_3 = 1800\,\text{K}$ ($\tau = 1/6$). The heat capacity ratio assuming air as the working fluid equals $\kappa = 1.4$. The pressure coefficient is considered in the range (0.6–1). The isentropic efficiencies are taken from [9]. The values used are $\eta_c = \eta_e = 0.97$. Two values of heat leak coefficient are used: 0.05 and 0.1.

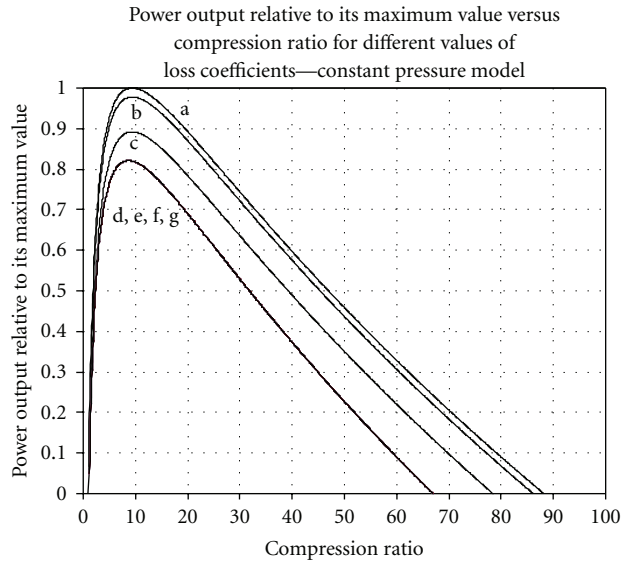

Figure 3: Relative power output to its maximum value versus compression ratio is plotted for different values of loss coefficients (pressure drop at point 1—ε_1, pressure drop at point 3—ε_3, compression isentropic efficiency—η_c, expansion isentropic efficiency η_e, and heat leak coefficient—k_{leak}). The loss coefficients' values are (in the same order appeared above) (a) 1, 1, 1, 1, 0; (b) 0.8, 0.8, 1, 1, 0; (c) 0.6, 0.6, 1, 1, 0; (d) 0.6, 0.6, 0.97, 0.97, 0; (e) 0.6, 0.6, 0.97, 0.97, 0.05; (f) 0.6, 0.6, 0.97, 0.97, 0.1; (g) 0.6, 0.6, 0.97, 0.97, 0.5.

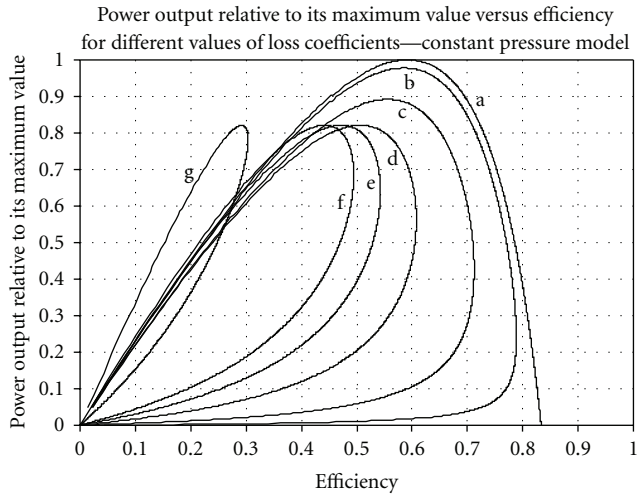

Figure 4: Power output relative to its maximum value versus efficiency is plotted for different values of loss coefficients (pressure drop at point 1—ε_1, pressure drop at point 3—ε_3, compression isentropic efficiency—η_c, expansion isentropic efficiency η_e, *and heat leak coefficient*—k_{leak}). The loss coefficients' values are (in the same order appeared above) (a) 1, 1, 1, 1, 0; (b) 0.8, 0.8, 1, 1, 0; (c) 0.6, 0.6, 1, 1, 0; (d) 0.6, 0.6, 0.97, 0.97, 0; (e) 0.6, 0.6, 0.97, 0.97, 0.05; (f) 0.6, 0.6, 0.97, 0.97, 0.1; (g) 0.6, 0.6, 0.97, 0.97, 0.5.

3.1. Constant Pressure Model. The performance characteristics of the constant pressure model are summarized in Figures 2–4.

Figure 2 shows the efficiency of the heat engine for different values of loss parameters as a function of the compression ratio. The ideal case is represented by the set of parameters $e1, e3, ec, ee, k_{\text{leak}}$: 1, 1, 1, 1, 0 ($e1$, $e3$, ec, ee, k_{leak} and are ε_1, ε_3, η_c, η_e, and k_{leak}, resp.). From Figure 2 one observes that the efficiency is reduced by 15% for pressure drop of 60% only, accounting for isentropic efficiency of 0.97, and heat leak reduces the efficiency to the level of 30%.

Figure 3 shows the normalized power output relative to its maximum value for the same set of parameters used in Figure 2. From the plot one observes that the maximum power output is reduced approximately by 12% due to 60% pressure only. Accounting for the other modes of losses, the maximum power output could reach the 40% level or even lower.

Figure 4 shows the same results of Figures 2 and 3 replotted using power efficiency coordinates. The normalized power output relative to its maximum value is plotted versus efficiency for different values of loss modes. The plot is very sensitive to the isentropic efficiency and heat leak. For isentropic efficiency of 0.97, the efficiency was reduced from 0.71 to 0.60 (15% reduction in efficiency). The efficiency is very sensitive to heat leaks too. For doubling the heat leak coefficient, the efficiency was reduced by 40%.

3.2. Reversible Adiabatic Expansion Model. The performance characteristics of reversible adiabatic expansion model are summarized in Figure 6.

Figure 6 shows the power output relative to its maximum value versus efficiency for different values of the pressure drop at the hot side (point 3). Both efficiency and power are reduced. From the figure it is obvious that the maximum power is very sensitive to this kind of assumption, while the efficiency is much less sensitive. The maximum efficiency is reduced by 13% approximately at the price of zero power.

3.3. Polytropic Expansion Model. The performance characteristics of the polytropic expansion process are summarized in Figure 7.

From the figure it is clear that both power and efficiency are very sensitive to the exponent n of the polytropic process. For 20% pressure drop, the maximum efficiency reduced to 65% (22% reduction) while the power relative to its maximum value is reduced to 0.8 (20% reduction).

4. Conclusion and Discussion

In this study the air standard Otto cycles were reconsidered to account for pressure drop. At first, different studies were reviewed. These studies considered different modes of losses including finite heat transfer rates, friction, heat leaks, internal irreversibility represented by the isentropic efficiencies, combustion efficiency, piston speed, and volumetric efficiency. The objective functions typically include maximizing power or maximizing efficiency. Some studies considered finding optimal paths leading to the maximum power or maximum efficiency of the Otto cycle. The pressure drop from simulations of realistic Otto cycle models was observed to be in the level of 60%.

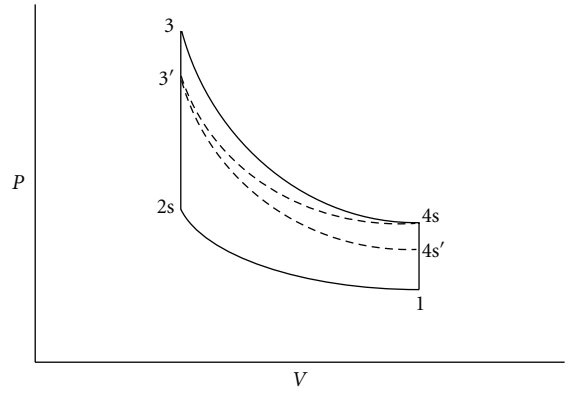

Figure 5: Schematics of the air standard Otto cycle with pressure drop from point 3 to 3′ and reversible adiabatic expansion and 3′ → 4s (reversible adiabatic model assumption), 3′ → 4s′ is a polytropic process (polytropic expansion model assumption).

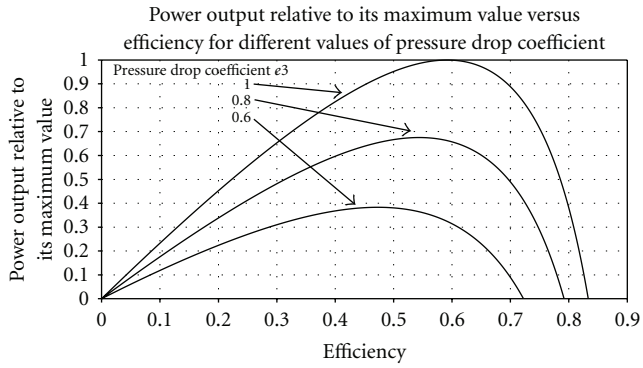

Figure 6: Power output relative to its maximum value versus efficiency for the reversible adiabatic model. Plots are shown for different values of the pressure drop coefficient ($e3$) at the hot side. The maximum efficiency is reduced but at zero maximum power production. Plots are shown for different values: $e3 = 1.0,\ 0.8,\ 0.6$.

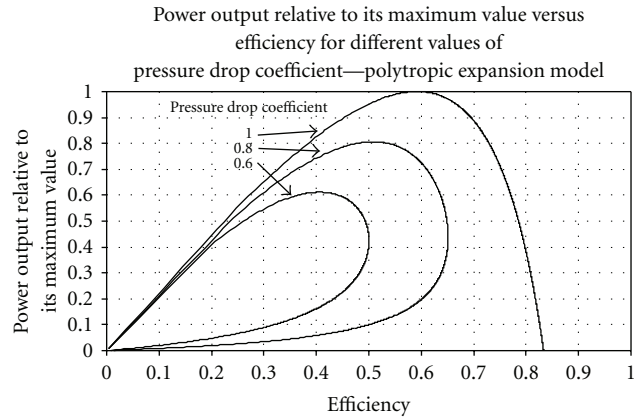

Figure 7: Power output relative to its maximum value versus efficiency for polytropic expansion model. Both efficiency and power are reduced drastically as a function of the pressure coefficient ($e3$). Plots are shown for three different values: $e3 = 1.0,\ 0.8,\ 0.6$.

Three different modeling assumptions are considered for the pressure drop: constant pressure model, reversible adiabatic expansion model, and polytropic expansion model.

The pressure drop as introduced in Section 2 is represented by a constant parameter. It was found that the efficiency was reduced by 15% approximately for 60% pressure drops based on the constant pressure model.

Two other modes of losses are included in constant pressure model: internal irreversibility and heat leak. From Figures 2–4 one observes that the efficiency is very sensitive to the internal irreversibility in the first place, then to heat leak, and lastly to pressure drop.

The reversible adiabatic model showed mild reduction in the maximum efficiency, but at that point the power output vanishes.

The last model considered in this study predicts strong reduction in the maximum efficiency (22% for 20% pressure drop and 40% for 40% pressure drop).

All three models show that the net power output is reduced in stronger fashion than that of the efficiency. It is important to note that heat leak as modeled in the first model does not affect the net power output.

References

[1] K. H. Hoffman, "Recent development in finite time thermodynamics," *Technische Mechanik*, vol. 22, no. 1, pp. 14–25, 2002.

[2] S. L. Harvey, "Thermal efficiency at maximum work output: new results for old heat engines," *The American Journal of Physics*, vol. 55, no. 7, pp. 602–610, 1987.

[3] M. Mozurkewich and R. S. Berry, "Optimal paths for thermodynamic systems: the ideal Otto cycle," *Journal of Applied Physics*, vol. 53, no. 1, pp. 34–42, 1982.

[4] L. Chen, C. Wu, F. Sun, and C. Shui, "Heat-transfer effects on the net work output and efficiency characteristics for an air-standard Otto-cycle," *Energy Conversion and Management*, vol. 39, no. 7, pp. 643–648, 1998.

[5] R. Ebrahimi, "Engine speed effects on the characteristic performance of Otto engines," *The American Journal of Science*, vol. 6, no. 1, pp. 123–128, 2010.

[6] B. M. Mehta and O. S. Bharti, "Performance analysis of an irreversible Otto cycle using finite time thermodynamics," in *Proceedings of the World Congress on Engineering (WCE '09)*, vol. 2, pp. 1–3, London, UK, 2009.

[7] M. N. Khan, "Alternative approach of irreversible Otto cycle," *International Journal of Engineering Science and Technology*, vol. 2, no. 6, pp. 1860–1866, 2010.

[8] R. Ebrahimi, "Effects of variable specific heat ratio on performance of an endoreversible Otto cycle," *Acta Physica Polonica A*, vol. 117, no. 6, pp. 887–891, 2010.

[9] R. Ebrahimi, "Theoretical study of combustion efficiency in an Otto engine," *The American Journal of Science*, vol. 6, no. 2, pp. 113–116, 2010.

[10] J. B. Heywood, *Internal Combustion Engine Fundamentals*, McGraw-Hill, New York, NY, USA, 1988.

[11] X. Qin, L. Chen, F. Sun, and C. Wu, "The universal power and efficiency characteristics for irreversible reciprocating heat engine cycles," *The European Journal of Physics*, vol. 24, no. 4, pp. 359–366, 2003.

[12] R. Ebrahimi, D. Ghanbarian, and M. R. Tadayon, "Performance of an Otto engine with volumetric efficiency," *The American Journal of Science*, vol. 6, no. 3, pp. 27–30, 2010.

[13] J. M. Gordon and M. Huleihil, "General performance characteristics of real heat engines," *Journal of Applied Physics*, vol. 72, no. 3, pp. 829–837, 1992.
[14] P. I. Curto-Risso, A. Medina, and A. C. Hernandez, "Theoretical and simulated models for irreversible Otto cycle," *Journal of Applied Physics*, vol. 104, article 094911, pp. 1–11, 2008.